PUBLICATIONS OF THE ASTRONOMICAL SOCIETY OF THE PACIFIC, **121**:174–184, 2009 February

The PLATO Dome A Site-Testing Observatory: Instrumentation and First Results

H. YANG,[1] G. ALLEN,[2] M. C. B. ASHLEY,[3] C. S. BONNER,[3] S. BRADLEY,[4] X. CUI,[5] J. R. EVERETT,[3] L. FENG,[6] X. GONG,[5] S. HENGST,[3] J. HU,[7] Z. JIANG,[7] C. A. KULESA,[8] J. S. LAWRENCE,[3] Y. LI,[1] D. LUONG-VAN,[3] M. J. MCCAUGHREAN,[9] A. M. MOORE,[10] C. PENNYPACKER,[11] W. QIN,[1] R. RIDDLE,[12] Z. SHANG,[13] J. W. V. STOREY,[3] B. SUN,[1] N. SUNTZEFF,[14] N. F. H. TOTHILL,[9] T. TRAVOUILLON,[10] C. K. WALKER,[8] L. WANG,[6,14] J. YAN,[6,7] J. YANG,[6] D. YORK,[15] X. YUAN,[5] X. ZHANG,[6] Z. ZHANG,[1] X. ZHOU,[7] AND Z. ZHU[6]

Received 2008 December 23; accepted 2009 January 26; published 2009 March 2

ABSTRACT. The PLATeau Observatory (PLATO) is an automated self-powered astrophysical observatory that was deployed to Dome A, the highest point on the Antarctic plateau, in 2008 January. PLATO consists of a suite of site-testing instruments designed to quantify the benefits of the Dome A site for astronomy, and science instruments designed to take advantage of the unique observing conditions. Instruments include CSTAR, an array of optical telescopes for transient astronomy; Gattini, an instrument to measure the optical sky brightness and cloud cover statistics; DASLE, an experiment to measure the statistics of the meteorological conditions within the near-surface layer; Pre-HEAT, a submillimeter tipping radiometer measuring the atmospheric transmission and water vapor content and performing spectral line imaging of the Galactic plane; and Snodar, an acoustic radar designed to measure turbulence within the near-surface layer. PLATO has run completely unattended and collected data throughout the winter 2008 season. Here we present a detailed description of the PLATO instrument suite and preliminary results obtained from the first season of operation.

Online material: color figures

1. INTRODUCTION

1.1. Motivation

For many years the Antarctic plateau has been recognized as offering an outstanding opportunity for astronomy (e.g., Storey 2005). The high altitude, low temperatures, minimal free-atmosphere turbulence, and a very thin surface layer combine to produce observing conditions that are unrivaled elsewhere on the planet.

Site testing spanning more than a decade, first at the South Pole and more recently at Dome C, has quantified the gains that an Antarctic observatory can enjoy (e.g., Storey et al. 2007). While there are technical and logistic challenges to be overcome, the success of major projects such as the South Pole Telescope (Ruhl et al. 2004; Staniszewski et al. 2008) has demonstrated that these challenges are not insurmountable, and that the expected gains can be realized in practice. Figure 1 shows the location of the existing stations on the Antarctic plateau: South Pole, Dome C, Vostok, and Dome F (operated by the US, France/Italy, Russia, and Japan, respectively) plus the new site of Dome A (currently being developed by China).

Mountaintops are often the preferred locations for an observatory. At higher elevations, less atmosphere remains above the telescope, the precipitable water vapor will be less, and the temperature will be colder. At temperature sites, however, higher elevations are also windier and often very difficult for all but goats or mountaineers to access.

On the Antarctic plateau, the advantages of a higher elevation increase even faster with altitude, as the low temperatures mean

[1] Polar Research Institute of China, Pudong, Shanghai 200136, China.
[2] Solar Mobility Pty Ltd, Thornleigh, NSW 2120, Australia.
[3] School of Physics, University of New South Wales, NSW 2052, Australia.
[4] Physics Department, University of Auckland, Auckland 1142, New Zealand.
[5] Nanjing Institute of Astronomical Optics and Technology, Nanjing 210042, China.
[6] Purple Mountain Observatory, Nanjing 210008, China.
[7] National Astronomical Observatories, Chinese Academy of Sciences, Beijing 100012, China.
[8] Steward Observatory, University of Arizona, Tucson, AZ 85721.
[9] School of Physics, University of Exeter, Exeter EX4 4QL, UK.
[10] Department of Astronomy, California Institute of Technology, Pasadena, CA 91125.
[11] Lawrence Berkeley National Laboratory, University of California, Berkeley, CA 94720.
[12] Thirty Meter Telescope Project, Pasadena, CA 91107.
[13] Tianjin Normal University, Tianjin 300074, China.
[14] Physics Department, Texas A&M University, College Station, TX 77843.
[15] Department of Astronomy and Astrophysics and Enrico Fermi Institute, University of Chicago, Chicago, IL 60637.

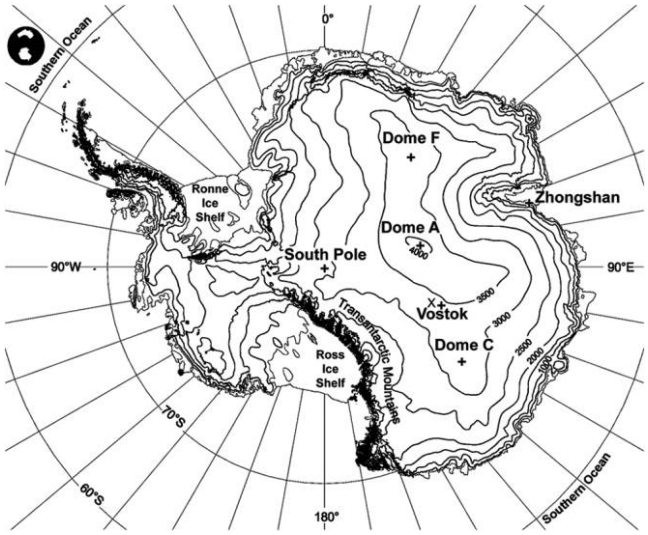

FIG. 1.—Map of Antarctica showing the Chinese coastal station Zhongshan and the high plateau stations South Pole, Dome C, Dome F, Vostok, and Dome A. *X*: current position of the south geomagnetic pole. Basic map courtesy of the Australian Antarctic Data Center.

that the scale height of the atmosphere is less than at temperate sites. In addition, because the wind patterns are predominantly katabatic (Parish & Bromwich 1987; Parish & Bromwich 2007), the surface wind speeds *decrease* as the altitude of the site increases. This, combined with still lower temperatures, implies that the stable boundary layer will be even thinner. Finally, because the topography of the Antarctic plateau is very smooth, access to the highest sites—though more challenging—is by a straightforward extension of the well-established traverse techniques used to reach the existing Antarctic plateau stations such as Dome C.

For all these reasons, the highest point on the plateau, Dome A, has been considered for many years to represent the ultimate observing site on the plateau, and hence the earth (Harper 1989; Gillingham 1991). The advantages are expected to be particularly strong in the far-infrared/submillimeter part of the spectrum, where the high altitude and low water vapor content can be expected to offer unparalleled transmission (Lawrence 2004).

1.2. Dome A

Dome A is a broad ridge with a change in elevation of only a few meters over an area of more than 100 km^2 (Liu et al. 2007; Zhang et al. 2007). The physical altitude is 4093 m, while the pressure altitude is typically 4600 m. It is ~1200 km from the nearest coastal stations (Davis and Zhongshan) and ~1100 km from the geographic south pole. It is currently about ~600 km from the geomagnetic south pole, placing it in a less favorable position with respect to the auroral oval than Dome C, but more favorable than South Pole or Dome F (Dempsey et al. 2005; Kenyon & Storey 2006).

The Dome A site was first visited, via overland traverse, in 2005 January by the Polar Research Institute of China (PRIC). The PRIC intends to establish a permanently manned station at Dome A within the next decade[16]. As part of this process they conducted a second expedition to Dome A, arriving in 2008 January, which involved the delivery and installation of the PLATeau Observatory (PLATO). This expedition, with scientific goals in fields including astronomy, glaciology, subglacial geology, climatology, and upper atmospheric physics, consisted of a 17-member team with a range of scientific equipment, transported by an over-ice tractor convoy. The traverse arrived at Dome A on 2008 January 11, after a 22-day journey from the Chinese Antarctic coastal station Zhongshan. The expedition spent 15 days at the Dome A site, during which time PLATO and its instrumentation suite were assembled and tested, before the team returned to the coast.

1.3. The PLATO Observatory

Site testing at any new site is always difficult. Once the logistic problem of getting there has been solved, there remain the challenges of providing power and communications, and of developing autonomous instruments that can operate unattended. Antarctica introduces additional challenges beyond those normally experienced at a "green field" site. Firstly, with servicing visits limited to once per year, the facility must be designed to be extremely reliable and robust. Secondly, with no access to grid power or other services, the observatory must be entirely self-sufficient for electrical power, thermal management, and satellite communications. Finally, there are special challenges presented by the Antarctic environment, including the very low temperatures, high altitude, and high relative humidity.

The development of automated stations for Antarctica has occurred over more than two decades. The best known are the Automated Weather Stations, of which more than 20 are currently operational across the East Antarctic plateau[17]. Additionally, both the United States Antarctic Program (USAP) and the British Antarctic Survey have developed (Dudeney et al. 1998) a number of Automated Geophysical Observatories (AGO) that are currently in operation[18].

Astronomical site-testing instruments are often complex and have a rather high power requirement, upwards of hundreds of watts. The amount of data acquired can be very large (on the

[16] See the *Final Comprehensive Environmental Evaluation* for the construction and operation of the Chinese Dome A Station in Antarctica prepared by the Chinese Arctic and Antarctic Administration at http://www.chinare.cn/en/.

[17] See, for example, the Antarctic Meteorological Research Center Website at http://uwamrc.ssec.wisc.edu/aws.html.

[18] See the United States Antarctic Program AGO Website at http://www.polar.umd.edu/ago.html.

order of terabytes), and optical systems must be protected from snow and frost. To support a program of site testing across the plateau, the University of New South Wales has developed a series of platforms over the past decade.

The first of these platforms, the Automated Astrophysical Site Testing Observatory (AASTO; Storey et al. 1996) was based closely on the USAP AGO. It used a propane-fueled thermo-electric generator (TEG) to generate some 50 W of electrical power and 2.5 kW of heat. AASTO was deployed initially to the South Pole, where it was used to test concepts for the later platforms. The second facility was the Automated Astrophysical Site Testing INternational Observatory (AASTINO; Lawrence et al. 2005). AASTINO used a combination of solar power and Stirling engines to generate around 500 W. It was deployed to Dome C prior to the year-round manned operation of the station, and provided the first wintertime measurements, demonstrating the outstanding quality of that site (Lawrence et al. 2004).

Development of a platform to support site testing at Dome A presented still further challenges. These considerations led to the development of PLATO (Lawrence et al. 2008). Compared to the earlier platforms, PLATO is required to operate at a higher altitude and to generate greater power. For these reasons, a redundant set of six diesel engines was chosen, supplemented by two banks of solar panels.

Figure 2 shows the PLATO installation at Dome A. PLATO consists of two separate modules: the engine module, which houses the primary power source (Hengst et al. 2008); and the instrument module, which houses the power electronics, the control and communication systems (Luong-Van et al. 2008; M. C. B. Ashley et al. 2009, in preparation), and the instruments. Solar panels are mounted externally. The two modules are separated by about 50 m; this keeps the instruments clear of the exhaust stream as there is no preferred wind direction at Dome A[19].

FIG. 2.—PLATO installation at Dome A. *Center left*: the instrument engine module, with Gattini instruments on roof and Pre-HEAT on the front wall. The 15 m anemometer tower is installed behind the instrument module; the CSTAR telescope is partially assembled in front of it. *Center right*: solar panel banks; *far right*: engine module. See the electronic edition of the *PASP* for a color version of this figure.

The PLATO power, control, and communication systems were successfully commissioned in late 2008 January during the Dome A expedition, before the instruments were installed. The system ran autonomously for 204 days, until mid-August (when the system lost power due to a suspected engine exhaust leak).

1.4. PLATO Instrumentation

The PLATO system uses a modular design that allows a number of independent and autonomous instruments to be installed. Instruments are mounted either on the instrument module roof or externally on the snow surface. Regulated and current-limited instrument power is provided by a central PLATO "power distribution" unit. Individual instrument control computers are mounted inside the (relatively) warm instrument module, and communicate with the PLATO "Supervisor" computers via a local Ethernet network. The Supervisor computers communicate via the Iridium satellite network, which allows a limited amount of instrument data ($\sim$20 MB day^{-1}) to be downloaded.

The instrumentation suite for the first season of PLATO operation included the following:

1. CSTAR: an array of optical telescopes for transient astronomy;
2. Gattini: two optical cameras determining the optical sky brightness and cloud cover statistics;
3. DASLE: an array of sonic anemometers measuring the meteorological conditions within the near surface layer;
4. Pre-HEAT: a submillimeter tipping radiometer measuring the atmospheric transmission and water vapor content, and able to image the Galactic plane in spectral lines;
5. Snodar: an acoustic radar designed to measure turbulence within the near surface layer.

Additionally, four external web cameras are installed on the PLATO instrument module roof. These are designed primarily for housekeeping purposes, i.e., to check on the snow and ice accumulation on instruments and surfaces, but they also provide valuable qualitative assessment of various aspects of the site conditions, e.g., cloud cover, wind strength and direction, and aurora[20]. The following sections of this article provide descriptions of each of the PLATO instruments, and their preliminary results.

[19] See the Australian Antarctic Division Dome A AWS website at: http://www.aad.gov.au/weather/aws/dome-a/index.html.

[20] See the PLATO Website for sample images at http://mcba11.phys.unsw.edu.au/~plato/platowebcams.html.

2. CSTAR

2.1. Instrument Aims

CSTAR (Chinese Small Telescope ARray) is composed of four telescopes with fixed orientation, each with a different optical filter, observing a $20\,\mathrm{deg}^2$ field centered on the south celestial pole (Yuan et al. 2008). Each telescope takes an image every 10–30 seconds throughout the Antarctic winter period. Such a high cadence on a single wide field, with multicolor photometry, will provide a valuable data set. There are a range of scientific objectives for this telescope in several fields of variable and transient astronomy. These include supernovae studies, gamma-ray burst optical afterglow detection, exoplanet detection (through transit and microlensing techniques), and variable star light curves and statistics. This data set will additionally provide site characterization of the optical sky background, cloud cover, and aurora.

2.2. Instrument Description

Each of the four CSTAR telescopes has an entrance pupil diameter of 145 mm (equivalent aperture of 100 mm due to the large central obstruction) and a f/1.2 focal ratio, giving a field of view of $\sim 4.5^\circ \times 4.5^\circ$. The optical design, shown in Figure 3, consists of a catadioptric objective with a spherical primary mirror, giving low chromatic aberration for such a compact telescope with a fast focal ratio and wide field. The first plano lens serves as window and filter. Three of the telescopes have a fixed filter, providing imaging in g, r, and i bands. The fourth telescope is filterless, giving wideband (400–900 nm) coverage. Each camera uses a 1k $\times$ 1k frame transfer CCD array (Andor DV435) with a pixel size of 13 μm. While the CCDs each have a Peltier cooling capability, they are operated passively, i.e., at the external ambient temperature.

The CSTAR design is particularly suited to Antarctic operation, having no moving parts. In order to keep the focus unchanged through a 100° range in temperature (from 20° to −80°C), both the optics and the structure use low thermal expansion materials: Zerodur and fused silica for the main optical components, and Invar for the telescope tubes. Each telescope tube is hermetically sealed and has an indium-tin oxide coating applied to the front window. This conductive coating can be used to provide ~ 10 W of heating per camera, which has proven to be very successful in avoiding snow and ice formation on the external windows. The inside of the telescope tubes were purged with pure nitrogen before shipping, to avoid ice formation on the internal optical surfaces. The camera tubes are installed in a steel enclosure, see Figure 4, with a top surface that is tilted $\sim 10^\circ$ toward the South Pole. This enclosure, which incorporates a vibration-resistant design for transportation (Gong et al. 2008), is installed external to PLATO on the snow surface, using a tripod mount.

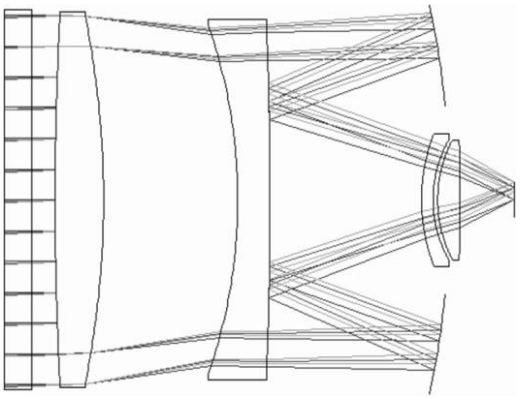

FIG. 3.—Optical design of CSTAR telescopes. This design results in 90% encircled energy within a two-pixel diameter. See the electronic edition of the *PASP* for a color version of this figure.

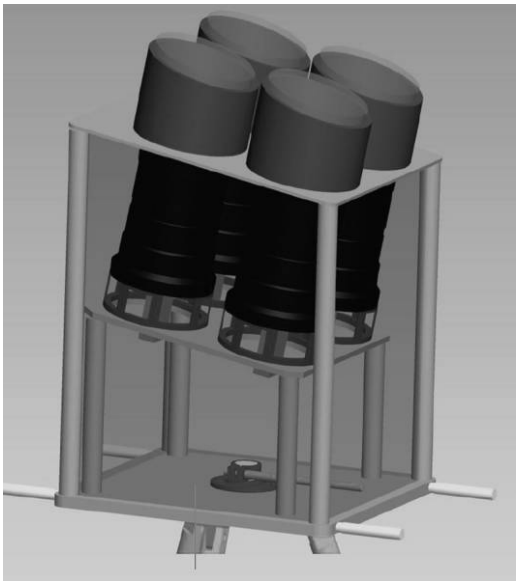

FIG. 4.—Model of CSTAR enclosure. See the electronic edition of the *PASP* for a color version of this figure.

Each camera has its own industrial computer with a wide working temperature range. Each computer uses a compact flash solid-state drive for the operating system and camera control software, and a 750 GB USB hard drive for data storage. Data collection, storage, and preliminary photometric analysis software for CSTAR are fully automated. While the majority of data will be retrieved during the next expedition (in early 2009), a subset of images and reduced data is returned each day via the PLATO Iridium network, allowing nominal operation of the instrument to be confirmed.

2.3. CSTAR Results

The CSTAR telescopes began taking data on 2008 March 17 when the sky became dark enough for stars to become visible.

i-band images were obtained on 115 of the 139 days between 2008 March 17 and 2008 August 2; the missing 24 days were due to difficulties in communicating with the CSTAR computer following emergency shutdowns to conserve power. Intermittent problems with the CSTAR computers and hard disks has meant that only the i-band data form a long data set.

An astrometric fit was performed on the i-band images using over 400 stars from the Tycho 2 catalog. The RMS residuals were 0.06 pixels, with low geometric distortion across the images. The CSTAR telescopes were aligned to the south celestial pole to an accuracy of better than 15′ (56 pixels on the images), and the individual telescopes were coaligned to better than 10′. The i-band images (Fig. 5) show excellent focus, with star images being 1.5 pixels full width at half-maximum (FWHM). The r-band and no-filter images showed evidence of some optical alignment problems, presumably due to vibration on the traverse to Dome A, and have FWHM of 4 and 2.5 pixels, respectively. No g-band images were obtained due to computer problems. The computer problems and optical alignment issues are being addressed during a servicing mission in 2009 January.

Data analysis (flat-fielding and aperture photometry) was performed in real time by the CSTAR computers at Dome A, and achieved residual noise of better than 3 millimags rms. Under clear conditions, typically 10,000 stars were measured per image. During the 115 days of operation, CSTAR transmitted 1.6 GB of reduced photometry data using the Iridium satellite link, and returned 488 of over 100,000 raw FITS images, each about 1 MB in size.

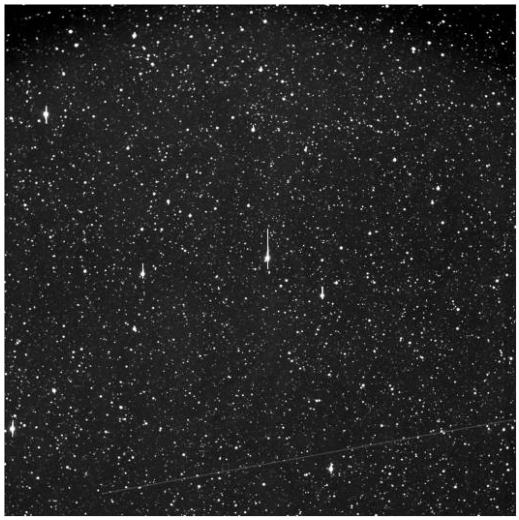

FIG. 5.—30-second i-band exposure taken on 2008 April 10 with the CSTAR1 telescope at Dome A. The field of view is $\sim 4.5° \times 4.5°$, centered to within 15′ of the south celestial pole. The image contains 1024×1024 pixels with a plate scale of 15.7″ per pixel. Stars down to an i magnitude of 14 are visible in this image. A satellite trail crosses the lower part of the image. More than half of the CSTAR images show such trails.

3. GATTINI

3.1. Instrument Aims

The percentage, duration, and intensity of dark time are critical values for ascertaining the quality of any astronomical site. It is expected that the optical sky conditions at Dome A will be distinctly different compared to high Antarctic plateau sites such as South Pole and Dome C (Dempsey et al. 2005; Kenyon & Storey 2006), and well-characterized midlatitude sites such as, for example, Cerro Paranal (Patat et al. 2006; Patat 2008); this has motivated the development of the GATTINI-Dome A instrument.

GATTINI was designed to: (1) measure the optical sky brightness at Dome A in a number of common astronomical wavebands as a function of solar and lunar zenith angle; (2) obtain accurate cloud cover statistics for the winter season; (3) obtain statistics on the spatial and temporal distribution of auroral events detected in astronomical filter bands; and (4) determine the variability of the wintertime atmospheric airglow due to hydroxyl line emission.

3.2. Instrument Description

The Gattini-Dome A instrument (see Moore et al. 2008 for technical details) is based on a similar instrument, Gattini-Dome C, that has operated successfully at Dome C station since 2006 (Moore et al. 2006, 2008).

Gattini comprises two separate cameras: the narrow-field Sky Brightness Camera (SBC), for the measurement of the optical sky background; and the wide-field All-Sky camera (ASC), for measurement of cloud cover, aurora, and airglow. Each camera is housed in a separate, sealed, thermally-regulated enclosure, which is mounted on the PLATO roof. Acrylic domes permit optical transmission and prevent external snow accumulation. Fans provide air circulation inside each enclosure to avoid internal ice formation. Both cameras use Apogee 2k × 2k interline USB CCD arrays, and contain four-element filter wheels. The cameras have fixed orientations; the SBC field is closely centered on the south celestial pole, and the ASC is observing toward zenith.

The SBC uses a 300 mm focal length Nikon lens (Nikon Telephoto AF-S Nikkor 300 mm f/4D ED-IF) with a 75 mm aperture giving a $2.8° \times 2.8°$ field of view sampled at 5″ pixel^{-1}. It contains Sloan g', r', and i' photometric filters in addition to an opaque mask (for dark current testing). Exposure times are nominally 20 s, equivalent to the time taken for a star to cross a single pixel at the edge of the field. The ASC uses a Nikon wide-field lens (10.5 mm f/2.8G ED AF DX Nikkor) with a focal length of 10.5 mm giving a pixel scale of 145.4″ pixel^{-1} and a field of view of $80° \times 80°$. The ASC filter wheel contains three Bessell filters (B, V, and R) and one long-pass red filter (RG665) for hydroxyl line emission redward of ~665 nm.

The Gattini cameras and DASLE experiment (see § 4) are jointly controlled by a Linux-based computer system. The control of all Gattini instrumentation is accomplished through a custom software suite. This fully autonomous software system controls the camera operation, dark correction, filter wheel drives, thermal regulation, hard drive management, data archiving, logging, and error correction. Data archiving is accomplished daily using a bank of four 500 GB hard drives.

3.3. Gattini Results

Gattini was installed on PLATO, and successfully passed system tests, during the two-week commissioning period at Dome A in 2008 January. The Gattini cameras were then activated remotely in 2008 late March. Although the Gattini control computer booted successfully at that time and images were obtained, a failure of the internal enclosure heaters meant that ice had formed on the enclosure domes. In mid-April, additional problems with the USB hard drive file system and the internal communication system required the Gattini instrument to be switched off. No useful site-testing data were thus obtained from the 2008 winter season.

A replacement ASC and control computer will be installed inside the PLATO module by the PRIC traverse team in 2009 January. The system has a redesigned enclosure requiring less heating, a conductive coating on the entrance window to prevent icing, and a redesigned and tested hard disk drive storage system. The Gattini ASC is a unique system for Dome A that provides information, e.g., cloud cover estimate and airglow variability, that is not available with the narrower field systems such as CSTAR and Gattini SBC.

4. DASLE

4.1. Instrument Aims

DASLE (Dome A Surface Layer Experiment) studies the meteorological conditions in the atmospheric boundary layer: measurements that are critical to the site evaluation of Dome A. The statistics of the wind speed and temperature in this layer are important for the design and performance of optical/infrared telescopes for several reasons (see, for example, Saunders et al. 2008a, Saunders et al. 2008b). Firstly, at other Antarctic plateau sites, wind shear within this layer creates most of the turbulence responsible for telescope image degradation. The vertical distribution of this turbulence thus determines the optimum height above the ground for telescope placement. Secondly, thermal fluctuations over time can lead to seeing degradation if there is a large mismatch (or lag) between the mirror (or telescope enclosure) temperature and the ambient air temperature. Thirdly, for an exposed telescope, the vertical thermal gradient results in a temperature differential across the primary mirror cell that can also lead to a degradation in image quality. Finally, variations in wind speed lead to wind shake and buffeting of the tower, telescope, and enclosure. The magnitude of these effects determines the degree to which they can be removed, e.g., by tip-tilt correction.

4.2. Instrument Description

DASLE is designed to measure the intensity and vertical extent of the boundary layer using three fast sonic anemometers. These instruments, manufactured by Apptech and modified for the Antarctic environment by the addition of heaters, measure temperature and 3D wind velocity from which the turbulence can be deduced (Skidmore et al. 2006). The sensors are mounted at three heights on a 15 m high tower that is installed ~10 m from the PLATO instrument module. The raw data rate of the anemometers is 200 Hz; after internal processing (compensation for aliasing and temporal and spatial averaging), the data streams from the three anemometers are synchronized electronically, and the wind components and temperatures are recorded at 20 Hz.

The DASLE experiment is controlled by the same Linux-based computer system that controls the Gattini instrument. Each day, DASLE data is automatically compressed and backed up, and a small sample of health and status data is sent through the PLATO system Iridium link. Like other metal structures, the anemometers are prone to ice formation. To remedy this problem, the anemometers are periodically switched off and heated by a resistance tape wrapped around the shaft and the transducer. Operation of similar instruments at Dome C over the past two winter seasons (Travouillon et al. 2008) has determined that a heating cycle of 20 minutes of each hour is appropriate to avoid ice formation and maximize data collection. In order to minimize the peak power consumption of the instrument, each anemometer is heated in turn.

4.3. DASLE Results

The DASLE tower and sensors were successfully installed at Dome A during the expedition, and data were collected during the first month of PLATO operation. This initial data set showed that the highest altitude sonic anemometer had been damaged in transit. Additionally, problems with the heater power supply system resulted in ice formation on the remaining two functional anemometers. An upgrade to the DASLE system to be installed in 2009 January by the PRIC traverse team will provide power and heating to a single anemometer at a height of 15 m.

5. PRE-HEAT

5.1. Instrument Aims

With significantly colder and drier conditions than both Mauna Kea and the Chilean Atacama desert, the high ice plateau of the Antarctic continent offers tantalizing prospects for astronomical observations at submillimeter wavelengths. Excellent results have been obtained from the (now-decommissioned) AST/RO telescope at the Amundsen-Scott South Pole Station

(Chamberlin 2002). The higher, drier, and colder conditions prevalent at Dome A are expected to be even better (Lawrence 2004)—notably opening up entirely new atmospheric windows at terahertz frequencies.

The Pre-HEAT instrument was developed for the PLATO observatory to characterize the submillimeter atmospheric conditions at Dome A. Pre-HEAT is a technological prototype for the High Elevation Antarctic Terahertz telescope (HEAT), and is comprised of a Schottky diode heterodyne receiver operating at a frequency of 660 GHz (450 μm wavelength) coupled to a 20 cm aperture single-axis telescope and a digital Fast Fourier Transform (FFT) spectrometer.

Pre-HEAT is designed with two principal scientific goals: to measure the 450 μm sky opacity over Dome A, and to perform spectral line observations of the Galactic plane in the ^{13}CO $J = 6 - 5$ line at 661 GHz. To achieve the same (10′) angular resolution of the landmark Columbia/CfA Galactic Plane CO $J = 1 - 0$ surveys (Dame et al. 2001), a 20 cm aperture is required at 660 GHz. The requirement of high-resolution spectroscopy combined with a tight power budget (<200 W) demands the use of an uncooled heterodyne receiver.

5.2. Instrument Description

A block diagram depicting the overall system architecture of the Pre-HEAT experiment is shown in Figure 6 (see Kulesa et al. 2008 for further technical details). The mechanical telescope assembly shown in Figure 7, which consists of two nested

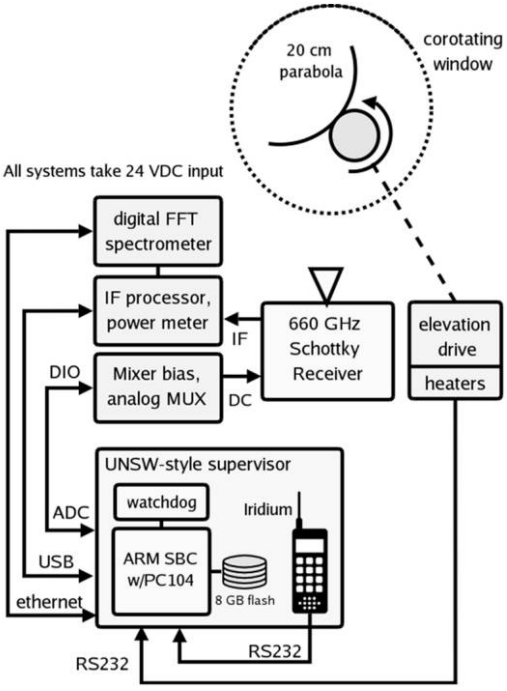

FIG. 6.—Block diagram of the Pre-HEAT subsystems. See the electronic edition of the *PASP* for a color version of this figure.

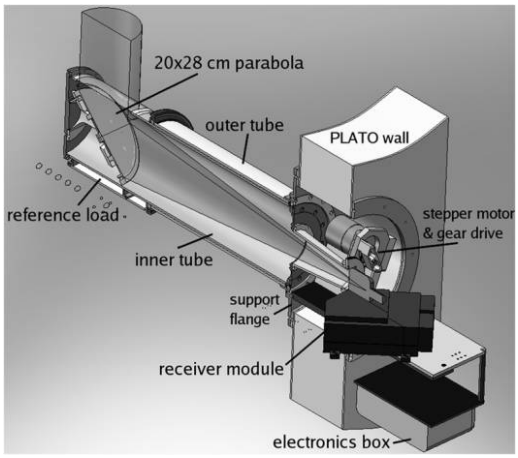

FIG. 7.—Cut-away schematic of the Pre-HEAT optical path and mechanical subassemblies. See the electronic edition of the *PASP* for a color version of this figure.

aluminum cylinders spaced by a pair of low-temperature ring bearings, is mounted through a port in the PLATO instrument module wall. A 0.4 mm thick sheet of HDPE serves as the entrance window, and a 20×28 cm 90° off-axis f/5 parabola mounted at one end of the cylinder serves as the primary mirror. A high-emissivity calibration load cell is attached to the bottom of the fixed outer tube. The load can be heated to two different temperatures in order to estimate the receiver noise temperature and gain, and is referenced by pointing the primary mirror downwards. The load cell is flanked by fixed nylon brushes which remove frost and snow accumulation as the telescope rotates.

The Pre-HEAT receiver module, which is located inside the PLATO instrument module, utilizes a fundamental planar-Schottky diode mixer receiver (Siegel et al. 1998) provided by P. Siegel at Caltech/JPL. A 656 GHz local oscillator signal is injected into the sky beam and brought to the receiver feed-horn by a folded Fabry-Perot diplexer. The resulting 2–12 GHz intermediate frequency (IF) is then amplified, down converted, and filtered to provide a 500 MHz-wide baseband signal for the FFT spectrometer. The FFT spectrometer board, constructed by Omnisys AB in Sweden, provides a total of 1 GHz of bandwidth in two IF channels for a total of 10 W of input DC power. The spectral output is sent over a serial RS-232 interface to Pre-HEAT's main single-board computer (based on a 200 MHz ARM9 processor) for subsequent processing and storage.

5.3. Pre-HEAT Results

Pre-HEAT was first powered at Dome A on 2008 January 14, and achieved first light on January 19. Manual operation of the instrument, using the Iridium network, proceeded from January 24 until the end of February. Autonomous operation followed in early March and continued until the PLATO shutdown in mid-August. The performance of the instrument is sufficient to

measure the sky opacity at 660 GHz, and initial spectra of ^{13}CO $J = 6 - 5$ are currently being analyzed and processed. Figure 8 shows an example of a Pre-HEAT skydip, and a model atmospheric spectrum for Dome A, using a precipitable water vapor concentration of 100 μm.

Measurements from Pre-HEAT represent the driest, clearest, and most stable submillimeter conditions ever seen from the ground—entire days with precipitable water vapor below ~100 μm have been measured. The best submillimeter conditions are expected in the July–September period. With such low water vapor and atmospheric pressure (560 mbar), entirely new terahertz atmospheric windows open, potentially allowing observations of [CII] at 158 μm (1.90 THz), [OI] at 145 μm (2.10 THz), and [OIII] at 88 μm (3.39 THz), in addition to the [NII] line at 205 μm (1.37 THz) already observed from Chile (Marrone et al. 2005) and the South Pole (Oberst et al. 2006). Ground-based observations of high-J transitions of the CO molecule and the ground state transition of the molecular ion H_2D^+ at 219 μm (1.37 THz) are also possible.

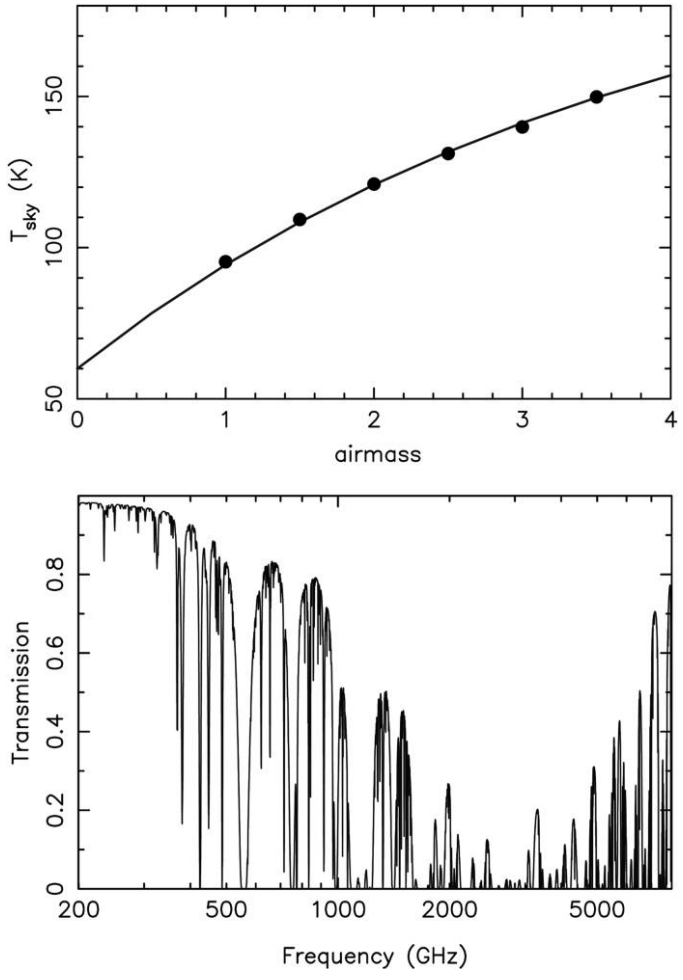

FIG. 8.—Example of Pre-HEAT data. *Top*: skydip (variation of sky brightness temperature with zenith angle); from this, we estimate a precipitable water vapor column of 100 μm. *Bottom*: Dome A atmospheric transmission spectrum for 100 μm of precipitable water vapor, modeled with the *am* (Paine 2004) code.

A future upgrade of the Pre-HEAT telescope to 50 cm aperture, combined with a complement of terahertz-frequency heterodyne receivers, would make these new far-infrared spectroscopic observations possible and extend the capabilities of ground-based submillimeter astronomy significantly. The exceptional submillimeter capabilities of sites like Dome A offer great promise for enabling new science and instrumentation technologies at submillimeter and terahertz frequencies.

6. SNODAR

6.1. Instrument Aims

The height, strength, and variability of the turbulence within the atmospheric boundary layer are of particular importance to astronomers since these factors directly affect the achievable image quality for large optical and infrared telescopes. The wind shear and thermal profiles throughout the Antarctic plateau atmosphere impart unique characteristics to the turbulent structure, from the ground layer to the troposphere.

The free atmospheric turbulence above the surface boundary layer has been found to be exceptionally calm and stable at Antarctic plateau sites such as the South Pole (Marks et al. 1999) and Dome C (Lawrence et al. 2004). Turbulence within the boundary layer at these sites, however, is known to be intense (Travouillon et al. 2003; Agabi et al. 2006; Trinquet et al. 2008). The turbulent boundary layer extends to a height of ~300 m at the South Pole; at Dome C, it is typically tens of meters thick. While data have yet to be obtained, simulations based on atmospheric and climate models predict that the wintertime turbulent boundary layer at Dome A will be weaker and confined closer to the surface (Swain & Gallée 2006), and that the high-altitude wind speeds will be weaker (Hagelin et al. 2008) than observed at other Antarctic plateau sites.

Snodar is a new instrument designed specifically to autonomously measure the height, strength, and variability of the atmospheric boundary layer at Antarctic plateau locations. Snodar's primary goal is to measure the atmospheric temperature structure function, C_T^2, from a height of 5 m up to at least 100 m, with a resolution of 1 m or better.

6.2. Instrument Description

The technique of measuring the temperature structure of the atmosphere with an acoustic radar was first demonstrated by Little (1969). The principle involves sending an intense acoustic pulse into the atmosphere and then listening for the faint scattering from temperature inhomogeneities. In order to sample the atmospheric temperature structure to a resolution of 1 m or better, the acoustic pulse must be 2 m in length or shorter (Tatarski 1971). This equates to a pulse length of 6.6 ms at an air temperature of -40°C, or just 33 cycles at the optimum operating frequency of 5 kHz.

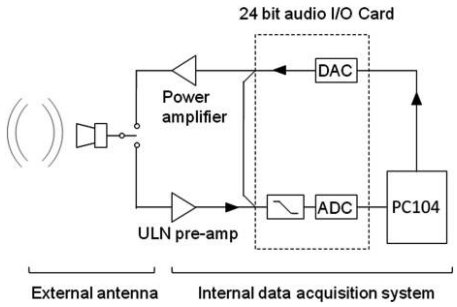

FIG. 9.—High-level overview of Snodar. The system is broken into two parts, the cold external components and the warm internal components. All analog IO is performed with a USB soundcard. Note the hardware loop back from the output to the input of the soundcard, allowing IO synchronization.

Figure 9 shows a high-level overview of Snodar. The instrument consists of a data acquisition system that is installed inside the warm PLATO instrument module, and a remote cold external acoustic antenna mounted on the snow surface ~15 m away (see Bonner et al. 2008 for more details).

The acoustic transducer, a horn-loaded compression driver (JBL2402H), has a frequency response from 2.5–15 kHz; the high operating frequency allows sharp pulses to be formed with minimal ringing. It is mounted at the focal point of a 1.5 m f/0.6 off-axis parabolic reflector. The transducer's radiation pattern is matched to the parabolic reflector f-ratio which results in a final beam width of approximately 4°. A 2.4 m tall "sound cone" is used to reduce acoustic background noise and fixed echoes. Electric heat pads, able to dissipate up to 200 W of power, are attached to the underneath of the parabolic reflector to stop the formation of frost and sublimate any accumulated snow or ice.

Signal processing and control functions are performed by a PC/104 running GNU/Linux (Debian etch) with a read-only root file system. A 24-bit external USB sound card is used for all analog signal IO. An ultra-low-noise preamplifier is used to amplify the faint echoes from atmospheric scattering to a usable level. A 60 W audio power amplifier amplifies the audio output of the USB soundcard, and an aerospace-grade electromechanical relay, specified to operate at temperatures down to −70°C, is used to switch the transducer between the power amplifier output and the preamplifier input. Snodar operates from a single 28 VDC supply with an average power consumption of <15 W.

6.3. Snodar Results

The functionality and operation of Snodar was confirmed during a testing period in Sydney before deployment. Complete system verification at such a temperate location is precluded by the high atmospheric attenuation at the instrument's nominal operating frequency of 5 kHz at temperatures above ~0°C. After a two-week commissioning period at Dome A, Snodar was remotely operational for several weeks, and a number of sampling schemes were employed. After this time, however, a suspected electromechanical relay failure resulted in the loss of transmit signal capability. Various modifications to Snodar are currently being designed in order to increase reliability. The electromechanical relay has been replaced with a solid-state solution that also replaces the audio power amplifier with an efficient class-D stage. These instrument upgrades will be installed during the summer 2008/2009 PRIC traverse.

The data collected from Dome A so far have demonstrated the feasibility of operating this instrument in the Antarctic environment. An example of Snodar raw (uncalibrated) data over a 48-hour continuous period is shown in Figure 10. Initial results are promising. For an operating frequency of 5 kHz, a spatial resolution of 1 m is obtained, consistent with design requirements. A strong diurnal variation in the turbulent boundary layer height and intensity is clearly observed. This is consistent with observations at Dome C, where a strong daily summertime

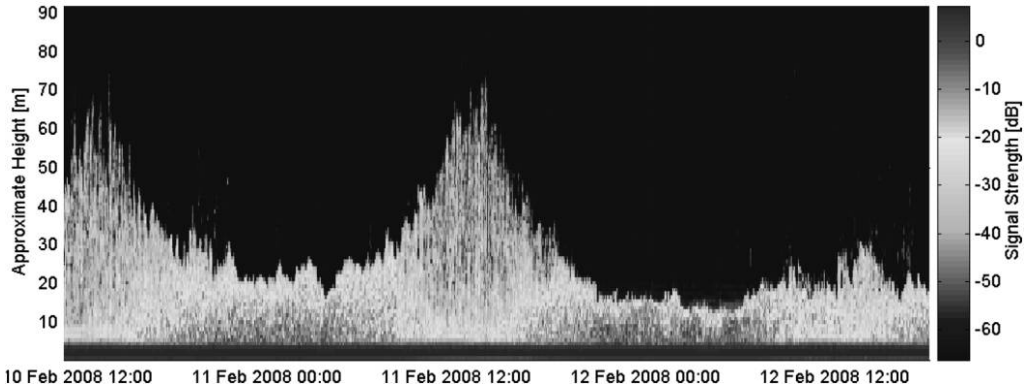

FIG. 10.—Fax plot of 48 hours of Snodar data. The operating frequency is 5 kHz, giving a spatial resolution of ~1 m. The strong signal in the first 8 m is from transducer ringing and enclosure reverberation. The raw (uncalibrated) signal strength shown here scales with the atmospheric temperature structure function, which is indicative of the strength of the turbulence. The sharp upper boundary layer is a real effect and shows a rapid (≤1 m) transition from the turbulent boundary layer to the nonturbulent air. See the electronic edition of the *PASP* for a color version of this figure.

variation in the integrated turbulence, i.e., seeing (Aristidi et al. 2005a), has been attributed to an oscillation of the surface thermal gradient between positive and negative (Aristidi et al. 2005b). Although data from midwinter are required, the observed height of the summertime turbulent boundary layer, which drops below ~20 m, is consistent with expectations (Swain & Gallée 2006). Additional work is now being conducted with the aim of achieving an absolute calibration of the Snodar return signal, in terms of C_T^2, by cross-comparison with a range of other site-testing instruments.

7. CONCLUSION

PLATO is an entirely self-powered observatory with a reliable, multiply-redundant, hybrid power-generation system. The command, control, and communications system for the observatory has proven robust against many potential failure points. This reliability has allowed PLATO to run unattended throughout the winter period in its first year of operation, and to collect the data that are crucial to quantify the Dome A atmospheric and environmental conditions in order to plan for larger scale future astronomical facilities at this site.

Preliminary data, presented here, from the first-generation PLATO instrument suite have indicated the potential of the Dome A site for astronomy. The Pre-HEAT instrument has shown that Dome A is likely to be the driest location on the planet, opening up new windows for terahertz astronomy. The CSTAR telescope array has demonstrated the potential for time-series astronomy from this location. The Snodar instrument has proven a novel instrument concept, and confirmed expectations of a low summertime turbulent boundary layer height. Further results from these instruments await the collection of the complete season of data from the next Dome A expedition.

Results from Gattini and DASLE, and wintertime results from Snodar, should be obtained during the 2009 season after planned upgrades to these instruments are implemented in the coming summer. There are also plans to extend the PLATO instrument suite to more fully characterize the site. Second generation instruments currently under development include Nigel, a fiber-fed optical spectrometer designed to measure the optical sky spectrum at various elevation angles (Kenyon et al. 2006); lunar SHABAR (Shadow Band Ranger), an array of photodiodes which measure the variation of lunar intensity to determine the profile of nighttime surface-layer turbulence (Hickson & Lanzetta 2004; Rajagopal et al. 2008); and MASS (Multi-Aperture Scintillation Sensor), an optical scintillometer which measures the atmospheric turbulence profile with low spatial resolution and high temporal resolution (Kornilov et al. 2003).

In the longer term, several larger-scale dedicated science facilities have been proposed to take full advantage of the unique Dome A site conditions now being demonstrated. These include HEAT (High Elevation Antarctic Telescope), a 0.5 m aperture submillimeter telescope designed to perform large-scale mapping surveys at the carbon, nitrogen, and oxygen fine structure and molecular lines (Walker et al. 2004); AST3 (Antarctic Schmidt Telescope array), an array of three 0.5 m wide-field optical Schmidt telescopes designed to obtain light curves for a large sample of Type Ia supernovae, and to search for exoplanets through gravitational microlensing (Cui et al. 2008); and Xian, an array of up to 400 fixed-position optical Schmidt telescopes, designed to find very large numbers of gamma-ray burst afterglows and supernovae (York et al. 2006; York 2008).

This research is supported by the Chinese PANDA International Polar Year project and the Polar Research Institute of China. The authors wish to thank all members of the 2008 PRIC Dome A expedition for their heroic effort in reaching the site and for providing invaluable assistance to the expedition astronomers in setting up the PLATO observatory and its associated instrument suite. A number of staff and students from the University of New South Wales provided valuable "last minute" contributions that helped to ensure the success of this project: we particularly thank George Georgevits, Mikayla Keen, Tim Leslie, and Jessie Christiansen. This research is financially supported by the Australian Research Council, the Australian Antarctic Division, the Chinese Academy of Sciences, the European Commission Sixth Framework Program, the National Natural Science Foundation of China, the US National Science Foundation, and the United States Antarctic Program. Additional financial contributions have been made by the institutions involved in this collaboration.

REFERENCES

Agabi, A., Aristidi, E., Azouit, M., Fossat, E., Martin, F., Sadibekova, T., Vernin, J., & Ziad, A. 2006, PASP, 118, 344
Aristidi, E., et al. 2005a, A&A, 444, 651
———. 2005b, A&A, 430, 739
Bonner, C., et al. 2008, Proc. SPIE, 7014, 70146I
Chamberlin, R. 2002, ASP Conf. Proc. 266, Astronomical Site Evaluation in the Visible and Radio Range, IAU Technical Workshop, ed. J. Vernin, Z. Benkhaldoun, & C. Muñoz-Tuñón (San Francisco: ASP), 172
Cui, X., Yuan, X., & Gong, X. 2008, Proc. SPIE, 7012, 70122D
Dame, T. M., Hartmann, D., & Thaddeus, P. 2001, ApJ, 547, 792
Dempsey, J. T., Storey, J. W. V., & Phillips, A. 2005, PASA, 22, 91
Dudeney, J. R., Kressman, R. I., & Rodger, A. S. 1998, Antarctic Science, 10, 192
Gillingham, P. R. 1991, Proc. Astron. Soc. Australia, 9, 55
Gong, X., Xia, L., & Zhang, R. 2008, Proc. SPIE, 7018, 701848
Hagelin, S., Masciadri, E., Lascaux, F., & Stoesz, J. 2008, MNRAS, 387, 1499
Harper, D. A. 1989, in AIP Conf. Proc. 198, Astrophysics in Antarctica, ed. M. Pomerantz (New York: AIP), 123

Hengst, S., Allen, G. R., Ashley, M. C. B., Everett, J. R., Lawrence, J. S., Luong-Van, D., & Storey, J. W. V. 2008, Proc. SPIE, 7012, 70124E
Hickson, P., & Lanzetta, K. 2004, PASP, 116, 1143
Kenyon, S. L., Ashley, M. C. B., Everett, J. R., Lawrence, J. S., & Storey, J. W. 2006, Proc SPIE, 6267, 6267M1
Kenyon, S. L., & Storey, J. W. V. 2006, PASP, 118, 489
Kornilov, V., Tokovinin, A., Vozyakova, O., Zaitsev, A., Shatsky, N., Potanin, S. F., & Sarazin, M. S. 2003, Proc. SPIE, 4839, 837
Kulesa, C., et al. 2008, Proc. SPIE, 7012, 701249
Lawrence, J. S. 2004, PASP, 116, 482
Lawrence, J. S., Ashley, M. C. B., & Storey, J. W. V. 2005, Australian J. Electrical Electron. Eng., 2, 1
Lawrence, J. S., Ashley, M. C. B., Tokovinin, A., & Travouillon, T. 2004, Nature, 431, 278
Lawrence, J. S., et al. 2008, Proc. SPIE, 7012, 701227
Little, C. G. 1969, Proc. IEEE, 57, 571
Liu, J., Wen, J., Wang, Y., Wang, W., Cathso, B. M., & Jezek, K. C. 2007, Chinese Geographical Science, 17, 160
Luong-Van, D. M., Ashley, M. C. B., Everett, J. R., Lawrence, J. S., & Storey, J. W. V. 2008, Proc. SPIE, 7019, 70192U
Marks, R. D., Vernin, J., Azouit, M., Manigault, J. F., & Clevelin, C. 1999, A&AS, 134, 161
Marrone, D. P., Blundell, R., Tong, E., Paine, S. N., Loudkov, D., Kawamura, J. H., Luhr, D., & Barrientos, C. 2005, Proc. ISSTT, eprint (arXiv:astro-ph/0505273)
Moore, A. M., et al. 2006, Proc. SPIE, 6267, 62671N
———. 2008, Proc. SPIE, 7012, 701226
Oberst, T. E., et al. 2006, ApJ, 652, L 125
Paine, S. 2004, SMA Technical Memo 152
Parish, T. R., & Bromwich, D. H. 1987, Nature, 328, 51
———. 2007, Monthly Weather Review, 135, 1961
Patat, F. 2008, A&A, 481, 575
Patat, F., Ugolnikov, O. S., & Postylyakov, O. V. 2006, A&A, 455, 385
Rajagopal, J., Tokovinin, A., Bustos, E., & Sebag, J. 2008, Proc. SPIE, 7013, 70131P
Ruhl, J., et al. 2004, Proc. SPIE, 5498, 11
Saunders, W., Gillingham, P., McGrath, A., Haynes, R., Brzeski, J., Storey, J., & Lawrence, J. 2008, Proc. SPIE, 7012, 70124F
Saunders, W., Gillingham, P., McGrath, A., Haynes, J., Storey, J., Lawrence, J., Burton, M., & Mora, A. 2008, Proc. SPIE, 7014, 70144N
Siegel, P. H., Mehdi, I., Dengler, R. J., Lee, T. H., Humphrey, D. A., Pease, A., Zimmermann, R., & Zimmermann, P. 1998, Microwave Symposium Digest, 2, 407
Skidmore, W., Travouillon, T., & Riddle, R. 2006, Proc. SPIE, 6267, 62671Z
Staniszewski, Z., et al. 2008, ApJ, submitted, eprint (arXiv:0810.1578)
Storey, J. W. V 2005, Antarctic Science, 17, 555
Storey, J. W. V, Ashley, M. C. B., & Burton, M. G. 1996, PASA, 13, 35
Storey, J. W. V., Lawrence, J. S., & Ashley, M. C. B. 2007. Revista Mexicana de Astronomia y Astrofisica Conference Series, 31, 25
Swain, M. R., & Gallée, H. 2006, PASP, 118, 1190
Tatarski, V. 1971, The Effects of the Turbulent Atmosphere on Wave Propagation, (Jerusalem: Keter Press)
Travouillon, T., Aristidi, E., Fossat, E., Lawrence, J., Mekarnia, D., Moore, A., Skidmore, W., & Storey, J. 2008, Proc. SPIE, 7012, 70124B
Travouillon, T., Ashley, M. C. B., Burton, M. G., Storey, J. W. V., & Lowenstein, R. F. 2003, A&A, 400, 1163
Trinquet, H., Agabi, A., Vernin, J., Azouit, M., Aristidi, E., & Fossat, E. 2008, PASP, 120, 203
Walker, C. K., et al. 2004, Proc. SPIE, 5489, 470
York, D. G. 2008, EAS Pub. Ser., 33, 225
York, D. G., et al. 2006, Proc. SPIE, 6267, 62671F1
Yuan, X., et al. 2008, Proc. SPIE, 7012, 70124G
Zhang, S., et al. 2007, Journal of Glaciology, 53, 159